Biogeosciences, 22, 1135–1147, 2025
https://doi.org/10.5194/bg-22-1135-2025

Biogeosciences Open Access EGU

A shift in circadian stem increment patterns in a Pyrenean alpine treeline precedes spring growth after snow melting

Helen Flynn[1,2], J. Julio Camarero[2], Alba Sanmiguel-Vallelado[3], Francisco Rojas Heredia[2], Pablo Domínguez Aguilar[2], Jesús Revuelto[2], and Juan Ignacio López-Moreno[2]

[1]Department of Geosciences, Colorado State University, Fort Collins, Colorado 80521, USA
[2]CryoPyr, Instituto Pirenaico de Ecología (IPE-CSIC), Zaragoza, 50059, Spain
[3]iuFOR, EiFAB, Universidad de Valladolid, Campus Duques de Soria, Soria, 42004, Spain

Correspondence: Helen Flynn (helen.flynn@colostate.edu) and Juan Ignacio López-Moreno (nlopez@ipe.csic.es)

Received: 30 October 2024 – Discussion started: 25 November 2024
Accepted: 13 January 2025 – Published: 28 February 2025

Abstract. Changing snow regimes and warmer growing seasons are some climate factors influencing the productivity and growth of high-elevation forests and alpine treelines. In low-latitude mountain regions with seasonal snow and drought regimes such as the Pyrenees, these climate factors could negatively impact forest productivity. To address this issue, we assessed the relationships between climate, snow, and inter- and intra-annual radial growth and stem increment data in an alpine *Pinus uncinata* treeline ecotone located in the central Spanish Pyrenees. First, we developed tree-ring-width chronologies of the study site to quantify climate–growth relationships. Second, radial growth, tree water deficit, and shrinking–swelling cycles were quantified and identified at monthly to daily scales using fine-resolution dendrometer data. These variables were extracted for three climatically different years, including one of the hottest summers on record in Spain (2022), and they were related to soil water content, soil and air temperature, and the dates of snow duration across the treeline ecotone. Warmer February and May temperatures enhanced tree radial growth, probably because of an earlier snow meltout, the start of the growing season, and the higher growth rates in spring, respectively. The characteristic circadian cycle of stem increment, defined by night swelling and day shrinking, was detected in summer and fall. However, this pattern was inverted during the snow season from November through April, suggesting a transition phase characterized by wet soils and swollen stems preceding the spring onset of growth. Air temperature, soil temperature and moisture, and the presence of snow are strong indicators of how much and for how long mountain trees can grow. Shifts in daily stem increment patterns reveal changes in early growth phenology linked to snow melting.

1 Introduction

In mountain areas, warming rates are much higher than in lowlands (Pepin et al., 2015), leading to changes in seasonal snow regimes and the soil moisture available for tree growth (Harpold and Molotch, 2015). Forest productivity and tree growth in high-elevation, subalpine forests and alpine treelines are especially sensitive to the warming effects of climate change (Albrich et al., 2020). However, drier conditions could also negatively impact low- to mid-latitude mountain forests, making the late-winter soil moisture coming from snow melting critical for tree growth. This has been observed in mountain areas subjected to strong snow and drought seasonality, such as the southern Rockies, the central Andes, and Mediterranean mountain ranges like the Pyrenees (Andrus et al., 2018; Saavedra et al., 2018; Vicente-Serrano et al., 2021; Villalba et al., 1994). High-elevation treeline forests are limited in productivity by climate variables like air and soil temperature (Peterson, 1998; Sanmiguel-Vallelado et al., 2021). Such forests are especially sensitive to the warming effects of climate change (Albrich et al., 2020) and can experience longer and, thus, more productive growing seasons (Yang et al., 2024).

Snow distribution and processes are clearly impacted by forest structures, but forests are also influenced by climate and snow. For instance, productivity was found to decrease

with a greater seasonal snow water equivalent (SWE) and later timing of meltout in the United States and southeastern Canada (Yang et al., 2024). Similarly, greater snowpacks led to less radial growth in mountain pine (*Pinus uncinata* Ram.) high-elevation forests in the Spanish Pyrenees (Sanmiguel-Vallelado et al., 2019), whereas monthly growth rates were found to be enhanced by a higher soil temperature linked to an earlier snowmelt (Sanmiguel-Vallelado et al., 2021). To make these different findings at yearly to monthly scales compatible, we need closer, fine-resolution approaches to understand how climate factors, and particularly snow dynamics, drive tree radial growth, which is a proxy of carbon uptake in woody tissues.

Snow is an essential water resource in the Spanish Pyrenees and is highly variable across the landscape, especially in the high-mountain treeline ecotone (Revuelto et al., 2017). Pyrenean forests have unique controls on snow distribution, redistribution, and sublimation that vary with forest density and structure (Hedstrom and Pomeroy, 1998; López-Moreno and Latron, 2008; Pomeroy et al., 2002; Revuelto et al., 2015; Storck et al., 2002). For this reason, it is important to gain a better understanding of how individual trees growing in alpine treelines respond to snowpacks. Snow and vegetation dynamics are being studied more often (Dobbert et al., 2022; Huang et al., 2023; Pomeroy et al., 2006; Sanmiguel-Vallelado et al., 2019, 2021; Yang et al., 2024), specifically in treeline ecotones, due to their relevance for forecasting future treeline shifts (Hagedorn et al., 2014; Huang et al., 2023).

The central Spanish Pyrenees range, due to its strong seasonality in snow cover and soil water availability during the growing season, provides an adequate setting for studying snow–forest interactions. In this area, treelines are dominated by mountain pine, which shows a growing season from May through October (Camarero et al., 1998). Radial growth rates of this species peak in May (Sanmiguel-Vallelado et al., 2021). In the Pyrenees, areas above 1600 m are snow-covered at least 50 % of the time from December through April, with wet soil and low temperature conditions (Gascoin et al., 2015). However, climate change is shifting the snow regimes in the Spanish Pyrenees, leading to a shorter snowpack duration due to a lower snow accumulation (López-Moreno, 2005; López-Moreno et al., 2020). Summer heatwaves and droughts are becoming common. This was illustrated by the summer of 2022, which was the hottest in the last several hundred years (Serrano-Notivoli et al., 2023; Izaguirre et al., 2024). In addition to increasing summer temperatures, climate change is increasing vapor pressure deficit (VPD), which could negatively impact forest productivity and growth by increasing the water evaporative demand (Noguera et al., 2023).

Trees swell and shrink throughout each day as a function of changes in soil moisture and atmospheric water demand, which are usually expressed as VPD. In late winter to early spring, usually from February to April, snow melts out and soils are wet, but later in the growing season higher temperatures dry soils and increase drought stress (Zweifel et al., 2016). During times of high heat and low soil moisture, trees can be impacted by drought stress, causing them to undergo reversible shrinking, which can be quantified through a metric called tree water deficit (TWD) derived from dendrometer measurements (Zweifel et al., 2016). Trees predominantly exhibit drought stress (high TWD) during daylight hours, which is why most radial growth occurs at night during the growing season (Zweifel et al., 2021). Tree stems shrink during the high-stress, TWD daylight hours, and they expand and contribute to irreversible radial growth during the cooler night hours. This mechanism for growth appears during the time of the year when it is advantageous for a tree to do so. Circadian approaches have been used to identify this trend in other biomes, with varying results. Some researchers have found that circadian clocks play an important role in triggering the onset of growth processes (Lázaro-Gimeno et al., 2024; Mei-Jun et al., 2023) and are influenced by environmental factors (Ziaco and Biondi, 2018), while others have had variable results (Lüttge and Hertel, 2009). Climatological conditions in the central Spanish Pyrenees vary greatly over the course of the year, which could cause a shift in daily circadian cycles.

If soil temperature and moisture, controlled by the presence of snow, drive the start of the growing season in high-mountain forests and alpine treelines (Sanmiguel-Vallelado et al., 2021), then soil temperature and the presence of snow dictate the magnitude and timing of tree growth in the treeline ecotone, with the shift being dictated by a change in the daily circadian rhythm of shrinking–swelling dynamics. The purpose of this research is to test this hypothesis and quantify the influence of varying climate and snow conditions on radial growth in a Pyrenean treeline ecotone at several timescales (year, month, day, and hour). To do this, we (1) compared tree growth and shrinking–swelling dynamics across three climatically differentiated years, (2) analyzed daily stem radius fluctuations as related to changes in growth and shrinking–swelling dynamics during warm and cold seasons, and (3) evaluated how climatic variables (air and soil temperature, snow, precipitation, and soil water content) affected growth and TWD.

2 Materials and methods

2.1 Study site

The study site is a relatively undisturbed treeline ecotone located in the Sierra de las Cutas (42.6371° N, 0.0512° W) near Ordesa y Monte Perdido National Park in northeastern Spain. The site is located at an average elevation of 2100 m facing 186° south-southwest and is dominated by mountain pine. The average slope is 17°, reaching a maximum of 33° when descending towards the forest. The soils are rocky and basic. The understory is dominated by several shrub species such

as *Juniperus communis* L. above the treeline and *Rhododendron ferrugineum* L. and *Calluna vulgaris* L. within the forest (Pardo et al., 2013).

2.2 Climate and dendrometer data

In an open area at the upper limit of the treeline, the automatic weather station (AWS) at Las Cutas is equipped to measure air temperature, relative humidity, wind velocity, and incoming solar radiation. The data from 2020 to 2024 were downloaded and processed, which revealed a gap in the sensor data from 6 December 2021 to 17 June 2022 due to battery malfunction (Fig. 1). There is a meteorological station 2 km away at the Góriz refuge (42.6634° N, 0.0148° E) with similar sensors, an additional precipitation gauge, and a snow depth sensor. In addition to the AWS at Las Cutas, there were four soil water content (SWC) sensors (ECH2O probe, model EC-5, Decagon Devices, Pullman, Washington, USA) installed at a depth of 10 cm in the forested zone of the treeline ecotone. One of the four sensors malfunctioned, so the SWC data were averaged across the three remaining sensors (Fig. 1). Other stand-scale climatological data were downloaded from the nearby Góriz refuge. The refuge lies on a similarly south-facing aspect at an elevation of 2200 m. The Góriz meteorological station provided additional daily air temperature, precipitation, and snow depth data. After correlating the existing daily minimum and maximum air temperature data from Las Cutas and the Góriz refuge, it was determined that the Góriz data could supplement the data from Las Cutas (Fig. A1).

In September 2020, stainless-steel-band dendrometers (DR 26, EMS Brno, Czech Republic) were placed on nine *P. uncinata* individuals in three zones of the treeline ecotone: forest (TRA), transition to the treeline (TRA-TRE), and treeline (TRE). The dendrometers recorded 15 min perimeter measurements at a high resolution of 1 µm and air temperature (T_{air}) until October 2024. The diameter at breast height (DBH) and the height were also measured for each individual tree (Table A1) when the dendrometers were installed in 2020. Radius values calculated using the perimeter measurements (assuming a spherical circumference) were then processed and cleaned using the treenetproc program in R (Knüsel et al., 2021). To examine the daily circadian rhythms of the trees, hourly stem radial increment values were calculated using the maximum hourly radius and then normalized across the nine individuals. Hourly stem radius values were then averaged by month across all the years to view the changes in daily shrinking and swelling patterns over the time period by month.

The soil temperature at each tree was recorded each hour using a combination of data loggers (Tinytag-Plus-2, model TGP-4017, Gemini Datalogggers UK Ltd., Chichester, West Sussex, UK; EasyLog-USB, model EL-USB-1 PRO, Lascar Electronics Ltd., Whiteparish, Wiltshire, UK; and Thermochron iButton, model DS-1922L, Dallas Semiconductors, Texas, USA). Data were downloaded and sensors replaced approximately every 6 months. Due to sensor malfunction, only six of the nine trees had a complete T_{soil} time series for the period of record. Extraneous T_{soil} values (greater than 100 °C away from 0 °C) were removed.

2.3 Tree-ring-width data and processing

In late October 2023, 20 mature trees were selected and two cores per tree were taken at 1.3 m using a Pressler increment borer. The cores were air-dried in the laboratory, glued to wooden mounts, and sanded with progressively finer sandpapers to visualize the tree-ring boundaries (Fritz, 1976). Then, they were scanned at 2400 dpi resolution and visually cross-dated under a stereoscope. Ring widths were measured at 0.001 mm resolution using scanned images and the CooRecorder-CDendro software (Maxwell and Larsson, 2021). The quality of the cross-dating was checked using the COFECHA software, which calculates moving correlations between individual series of ring-width values and the mean site series (Holmes, 1983).

To calculate climate–growth relationships, first the individual ring-width series were detrended by fitting x-year cubic smoothing splines with a 50 % frequency response cutoff, where x was two-thirds of the mean series length. The measured ring-width values were divided by fitted values. The resulting dimensionless ring-width indices were prewhitened by fitting autoregressive models and were averaged using biweight robust means. This allowed a mean series or chronology of ring-width indices to be compiled that preserved annual to decadal variability. Lastly, calculated over the common 1970–2023 period, an expressed population signal (EPS) ≥ 0.85 indicated a high common signal of the chronology (Wigley et al., 1984). These are the statistics characterizing the chronology (values are means $\pm$ SD): ring width $= 1.65 \pm 0.46$ mm, first-order autocorrelation $= 0.71 \pm 0.17$ mm, mean sensitivity of standardized width indices $= 0.24 \pm 0.05$ mm, and rbar $= 0.37$ mm. Lastly, Pearson correlations between the climate data and the ring-width indices were calculated from the previous September to the current September. Monthly climate data (Tx, mean maximum temperature; Tn, mean minimum temperature; and Pr, precipitation) were obtained from the 0.1° gridded E-OBS dataset v29.0e (Cornes et al., 2018) for the period 1970–2023. These procedures were carried out using the dplR (Bunn et al., 2023; Bunn, 2008, 2010) and treeclim (Zang and Biondi, 2015) R packages.

To verify that the patterns identified in the aforementioned methods were consistent with the Las Cutas experimental site, monthly correlations between climate variables (Tx, Tn, and Pr) and the mean series of ring-width indices (period 1970–2023) were calculated using the Pearson method for the September prior to the growing season of interest and up until the September after the growing season of interest. The results of that analysis were used to identify which climate

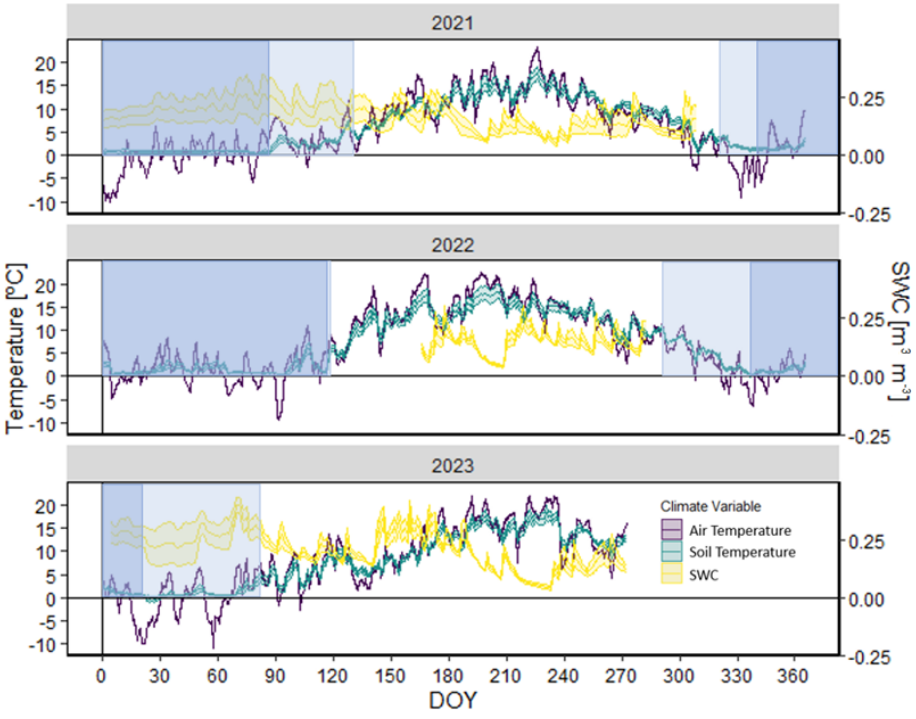

Figure 1. Daily mean air (T_{air}) and soil (T_{soil}) temperatures and mean soil water content (SWC) in the 3 study years. The values are means ± SE. Snow cover dates are outlined in vertical blue boxes with inconsistent snow cover defined by light blue and consistent snow cover defined by dark blue.

variables during which months showed the highest correlation with growth. Using that information, climate summaries from the months deemed influential were compared across the years to identify possible interannual variability and test the hypothesis.

2.4 Relating climate and dendrometer data

Daily stem radial increment time series were calculated from the sub-hourly dendrometer data using the maximum daily radius following a daily approach (Deslauriers et al., 2007). The growing season was defined as day of year (DOY) 100 through DOY 300 (Camarero et al., 1998; Sanmiguel-Vallelado et al., 2021). Using the daily radial increment data, the daily growth rate and the TWD were extracted from the time series (Zweifel et al., 2016). The correlation between the daily T_{air} and the growth rate was calculated during the growing period for values from the same day as well as a lagged correlation between the growth rate and T_{air} from the previous day up to 10 d before using the Pearson method. This correlation was also calculated between the SWC and TWD. In addition, 20 d moving correlations were calculated for the daily T_{air} and the growth rate, the daily T_{soil} and the growth rate, and the SWC and the TWD. This set of robust and simple statistics was useful for dealing with nonparametric analyses and was selected due to the small sample size of trees.

With the complete T_{soil} data, daily temperature oscillation (DTO) was calculated by subtracting the daily minimum temperature from the daily maximum temperature. A novel approach was used to determine the time periods in which snow was present. First, days with snow cover were identified using two different thresholds: a maximum DTO (DTOmax) of less than 2° or less than 5°. These two datasets for each of the six trees with T_{soil} data were used to define the snow cover duration periods. Snow cover was considered intermittent (IS), starting on the first date with snow presence and before the continuous (CS) period, which was defined as the period with gaps of less than 1 d. When gaps larger than 1 d began to occur again in the spring, the inconsistent period resumed until gaps with snow cover exceeded 15 d.

Because of the similar locations, climatological conditions, and strong correlations between the T_{air} recorded at the Góriz refuge and the AWS at Las Cutas (Fig. A1), the calculated snow cover duration dates were compared with the Góriz refuge snow depth data. Although the refuge sits at an elevation approximately 100 m higher than the Las Cutas average, the dates corresponded to accumulation and melting patterns identified in the Góriz snow depth data. The snow cover duration dates with a DTOmax of less than 2 were determined to be more accurate and were used for the rest of the analysis.

Table 1. Summary statistics of each growing season. All values are averages ± SE. Different letters indicate significant ($p < 0.05$) differences between the years according to the t tests.

Variables	Year		
	2021	2022	2023
Growth start (DOY)	151 ± 3a	143 ± 2b	136 ± 2c
Growth end (DOY)	249 ± 2a	287 ± 5b	244 ± 2a
Growth length (d)	83 ± 4a	144 ± 5b	108 ± 3c
Maximum growth rate (µm d^{-1})	19.7 ± 3.1	24.7 ± 2.4	22.7 ± 2.1
Date of maximum growth rate (DOY)	167 ± 2a	157 ± 3b	152 ± 3b

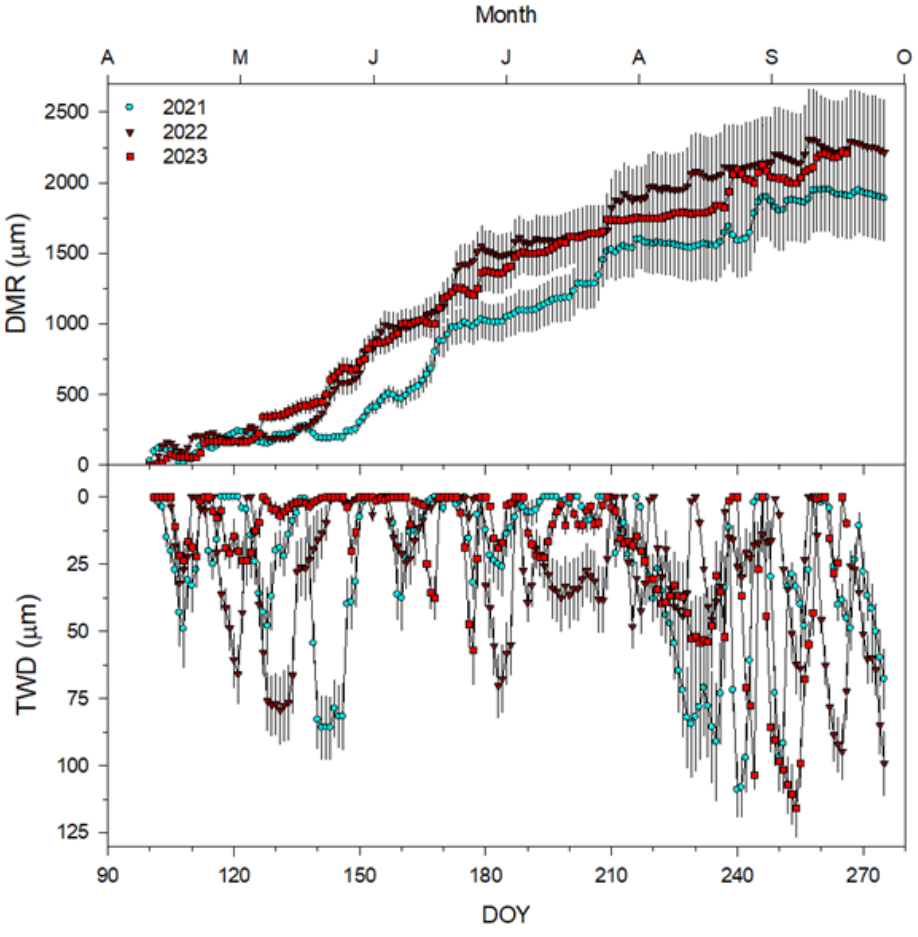

Figure 2. Daily values (means ± SE) of the radial stem variation (DMR) and minimum tree water deficit (TWD) in the 3 study years. DOY is the day of the calendar year.

3 Results

Each year of the study period showed varying tree growth and shrinking–swelling dynamics. In 2021, the onset of the growth and day of the maximum growth rate were slightly delayed compared to the other 2 years in which the maximum growth rate occurred, i.e., 10 d earlier in 2022 and 15 d earlier in 2023 on average (Table 1). In addition, the length of the 2021 growing season was shortest at an average of 83 d, while the 2022 season was longest at an average of 144 d (Table 1).

The average DMR in 2022 and 2023 showed increased growth rates starting around DOY 130. The 2022 growing season was the most gainful (approximately 2300 µm) of the three examined, while the 2021 season showed the least total growth (approximately 1900 µm) (Fig. 2). The TWD also varied in timing between the years. During the 2022 growing season, there were two large peaks (greater than 60 µm) be-

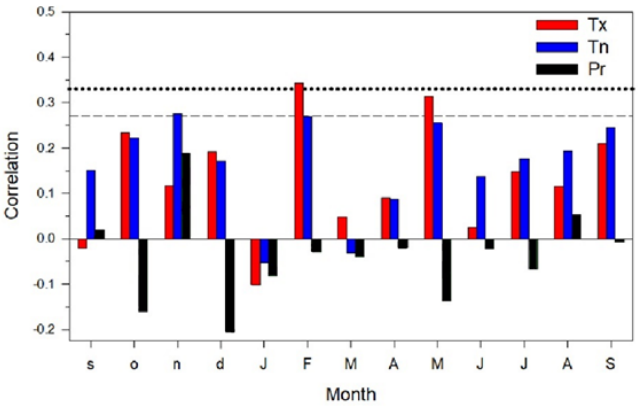

Figure 3. Climate–growth relationships (Pearson correlations) calculated by relating monthly climate variables (Tx, mean maximum temperature; Tn, mean minimum temperature; and Pr, total precipitation) to the mean series of ring-width indices (period 1970–2023). Correlations were calculated from September of the previous year (months abbreviated by lowercase letters) to September of the current year (months abbreviated by uppercase letters). Dashed and dotted horizontal lines show the 0.05 and 0.01 significance levels, respectively.

fore DOY 140 (Fig. 2). There was also one large peak in the TWD in 2021 around DOY 140 and DOY 225 (Fig. 2).

The TWD had high intra- and inter-annual variability throughout the time series (Fig. 2). There were small peaks in the TWD (less than 100 µm) around DOY 145 and DOY 130 in 2021 and 2022, respectively (Fig. 2). However, the largest peaks occurred in the late growing season between DOY 225 and DOY 280, with 2023 demonstrating the largest peak (Fig. 2).

Based on climate–growth correlations, the mean maximum air temperature and mean minimum air temperature from the months of February and May showed the highest correlation with growth indices (Fig. 3). Thus, climate summaries were compared across the years for these months and the overall growing season (Table 2).

The average air temperatures in February, May, and the fixed growing season (DOY 100 to DOY 300) were highest in 2022 and then in 2023 (Table 2). For instance, in 2021, 2022, and 2023, the growing season T_{air} values were 10.0, 12.4, and 12.0 °C, respectively. This was also true of the average soil temperatures, except for the fixed growing season in 2023, which had average soil temperatures of slightly less than 1 °C higher than in 2022 (Table 2). For instance, in 2021, 2022, and 2023, the growing season T_{soil} values were 9.9, 10.5, and 11.4 °C, respectively. Due to SWC sensor malfunction in 2022, data are limited to the fixed growing season. The average SWC was slightly higher in February, May, and the fixed growing season of 2023 than 2021 (Table 2). However, the SWC values were very similar despite the differences in T_{air}, T_{soil}, and precipitation for those 2 years.

Precipitation from the Góriz refuge also varied greatly between the first 2 years of this study. In 2021, the cumulative precipitation in February was 1102 mm (Table 2). This dropped to 51.0 mm in 2022 and then rose in 2023 for a total of 79.0 mm (Table 2). Similar trends were observed in May as well (Table 2). However, the total precipitation values for the entirety of each growing season were 684.4, 944.7, and 1140.1 mm for the years 2021, 2022, and 2023, respectively (Table 2).

Although snow presence was not directly recorded, days with snow were estimated using soil temperature. The longest consistent snow season occurred during the 2020–2021 winter, followed by 2021–2022 and, finally, 2022–2023 (Table 3). Unlike the other 2 years, which appeared to have a longer period of inconsistent snow towards the end of the winter, the 2021–2022 winter snow cover ended abruptly around DOY 118 ± 1, which was earlier than the 2020–2021 winter (DOY 128 ± 11) and later than the 2022–2023 winter (DOY 84 ± 5) (Table 3).

The moving correlations between T_{air} or T_{soil} with the growth rate showed generally similar patterns for the fixed growing seasons during the years 2021 and 2022 (Fig. 4). Both years had a window with a peak in positive significance for both T_{air} and T_{soil} during May (Fig. 4). This pattern appears to have occurred earlier in 2023, with the peak in significance already beginning to decline by the start of May. The year 2023 also stands out as the year with the smallest difference between T_{air} and T_{soil}.

The in-depth analysis of the seasonal changes in stem shrinking and swelling showed that the daily pattern shifts across the seasons (Fig. 5). The growing season pattern shows swelling during the evening and shrinking during the day, beginning in July or August and ending in November (Fig. 5). However, the pattern that can be seen during the snow season (November or December through April) is inverted, meaning that it is often the reverse of the normal growing season daily pattern, exhibiting swelling during the day and shrinking during the night (Fig. 5). The switch from the inverted pattern to the normal pattern occurred very rapidly during the months of May or June, as shown by the decoupling of the cycle between the trees (Fig. 5).

4 Discussion and conclusions

The onset of the growing season at this site is triggered by rising air and soil temperatures as well as the disappearance of the winter snowpack, which is consistent with previous studies conducted on the study species (Galván et al., 2014; Tardif et al., 2003). SWC was not identified as a strong indicator of the length of the growing season or the total growth. However, the data were limited due to the malfunctioning sensor during the late winter and onset of the growing season in 2022, which was a critical time period in the study. While important, May air and soil temperatures were less signifi-

Table 2. A summary of the climate variables at the study site and precipitation from the nearby Góriz station. Values are means ± SE.

Climate variable	Time period	2021	2022	2023
Soil temperature (°C)	February	0.73 ± 0.45	1.72 ± 0.55	0.84 ± 0.24
	May	5.88 ± 0.27	8.77 ± 0.79	7.12 ± 0.57
	Growing season	9.89 ± 0.52	10.54 ± 0.86	11.45 ± 0.66
Air temperature (°C)	February	1.14 ± 0.47	2.5 ± 0.57	0.06 ± 0.82
	May	6.22 ± 0.63	10.41 ± 0.82	6.7 ± 0.6
	Growing season	10.00 ± 0.37	12.39 ± 0.37	12.04 ± 0.39
SWC ($m^3\ m^{-3}$)	February	0.20 ± 0.01	–	0.25 ± 0.01
	May	0.18 ± 0.01	–	0.21 ± 0.01
	Growing season	0.15 ± 0.01	0.15 ± 0	0.18 ± 0.01
Precipitation (mm)	February	110.2	51.0	79.0
	May	104.4	21.6	118.0
	Growing season	684.4	944.7	1140.1

Table 3. Calculated snow season dates are included with IS, meaning the intermittent snow season, and CS, meaning the continuous snow season.

Snow season index	2021	2022	2023
IS_{start} (DOY)	275 ± 1	320 ± 4	292 ± 1
CS_{start} (DOY)	331 ± 4	339 ± 8	334 ± 7
CS_{end} (DOY)	87 ± 5	117 ± 49	22 ± 15
IS_{end} (DOY)	128 ± 11	118 ± 1	84 ± 5
Length of CS (d)	121 ± 9	113 ± 26	64 ± 15
Length of IS (d)	218 ± 11	163 ± 3	157 ± 5
Days w/ snow during IS (d)	156 ± 13	119 ± 13	106 ± 11
Percentage IS with snow	0.72 ± 0.06	0.73 ± 0.08	0.68 ± 0

cant when correlated with total growth than February air and soil temperatures. In winters like 2022 that were warmer in February, there was likely less precipitation falling and accumulating as snow, which leads to an earlier meltout date, earlier warming of the soil, and longer growing seasons that result in more total growth. In a previous study, February was identified as an important month in the climate–growth relationships, specifically between air temperature and radial growth (Sanmiguel-Vallelado et al., 2019). Additionally, researchers found that radial growth in *P. uncinata* was related to early and late growing season soil temperatures (Sanmiguel-Vallelado et al., 2021). They specifically found that May climatological conditions were more strongly correlated with growth than other months (Sanmiguel-Vallelado et al., 2021).

The high interannual variability of this region allows for the comparison of the impact of climatological differences on *P. uncinata* growth and TWD. Higher February air and soil temperatures in 2023 and especially in 2022 led to an earlier growth onset and a longer growing season, which is consistent with the findings in Sanmiguel-Vallelado et al. (2019). In summer, the central Spanish Pyrenees become hotter and drier, leading to high VPD and increased TWD. Under this set of environmental conditions, trees tend to close their stomata in order to conserve water during the hottest hours of the day (Grossiord et al., 2020). For this reason, it is common for trees to grow at night and in the early morning during months when the VPD and TWD during the day are too high (Tumajer et al., 2022; Zweifel et al., 2016). The normal growing season pattern was identified in previous research (Lázaro-Gimeno et al., 2024; Zweifel et al., 2016) and occurs during the warm months at Las Cutas, beginning in July or August and ending in October or November. This pattern could be due to normal responses to high VPD. During the cold months, when trees were not experiencing high VPD and had much lower daily growth rates, radial increment swelling occurred during the daylight hours. This switch in the swelling–shrinking cycle was attributed to the presence of snow, which was influenced by winter air temperatures and led to cold and moist soil conditions.

These findings could have implications for other high alpine treeline ecotones, especially in the Mediterranean region. Impacts of climate change like increasing winter and summer temperatures as well as snow accumulation and meltout will likely alter the timing of the growing season and impact growth and productivity, as clearly demonstrated by

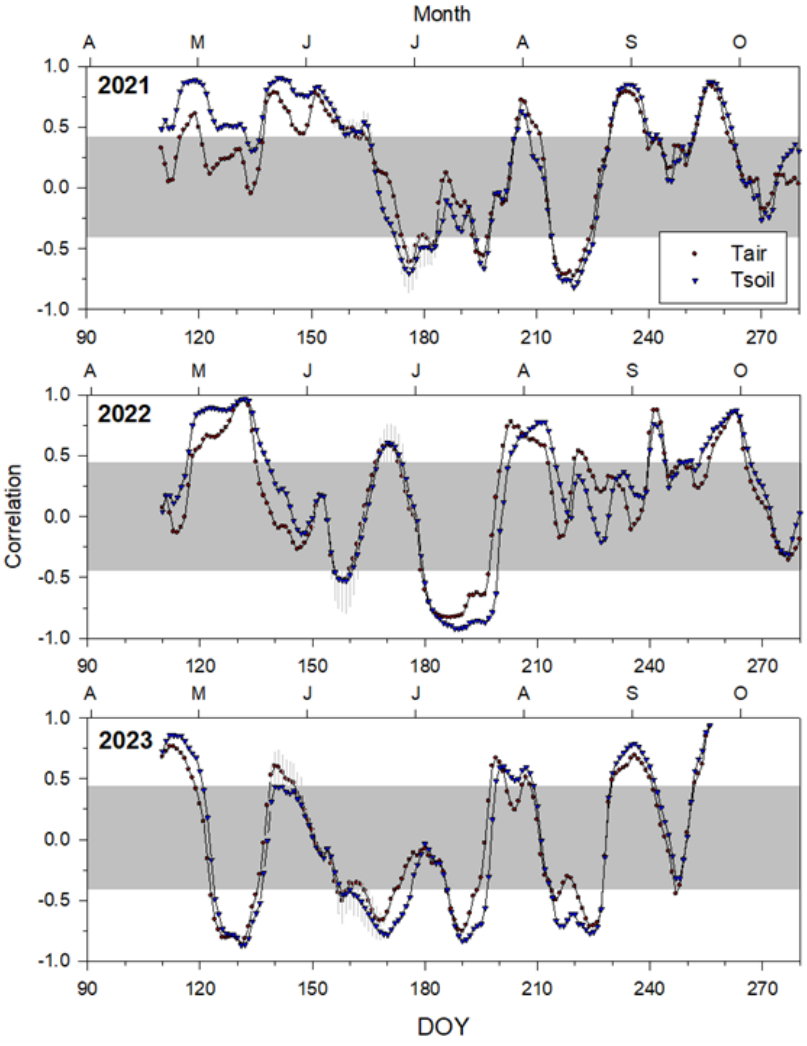

Figure 4. Moving correlations calculated by correlating air (T_{air}) or soil (T_{soil}) temperatures with daily growth rates along 20 d periods. Values are means ± SE. Correlation values located outside the grey box are significant ($p < 0.05$).

the year 2022 highlighted in this study (Table 1, Fig. 2). An overall increase in productivity could lead to greater carbon sequestration during the growing season, specifically in high-elevation areas of the Pyrenees that were previously agricultural lands but are now transitioning back to forests, either naturally or through afforestation efforts (Khorchani et al., 2022). The growing season at Las Cutas is limited by cold temperatures and the presence of snow, which causes the trees to remain in the inverted circadian pattern for longer (Fig. 6). However, in other, more arid mountain regions, warmer and drier conditions may lead to a longer growing season but amplify drought stress, which could limit carbon sequestration by reducing the rate of wood cell production (Ren et al., 2019).

It is important to acknowledge the limitations of this study. The sample size of the dendrometer data was small and the trees corresponded to a narrow range of ages, not allowing for widespread spatial and ontogenetic variability to be included. This is not ideal, especially in a treeline ecotone which experiences diverse and heterogeneous climate variability. Additionally, the presence of snow was determined using a novel method and a small sample size. However, overall snow accumulation patterns were confirmed using data from the nearby Góriz refuge. There is likely some error associated with these data, but, for the purposes of this study, we believe that the methods are useful and justified.

Future research could use in situ and short-range remotely sensed snow observations to confirm that snow is the driver of the changes in the growing season and the total growth that we saw in this study. Different locations of each tree (within the stand, outer edge, or krummholz) could also impact the timing of the snowmelt, growth rate, total growth, TWD, and circadian stem increment cycles. This is very relevant because the study's treeline ecotone is rapidly encroach-

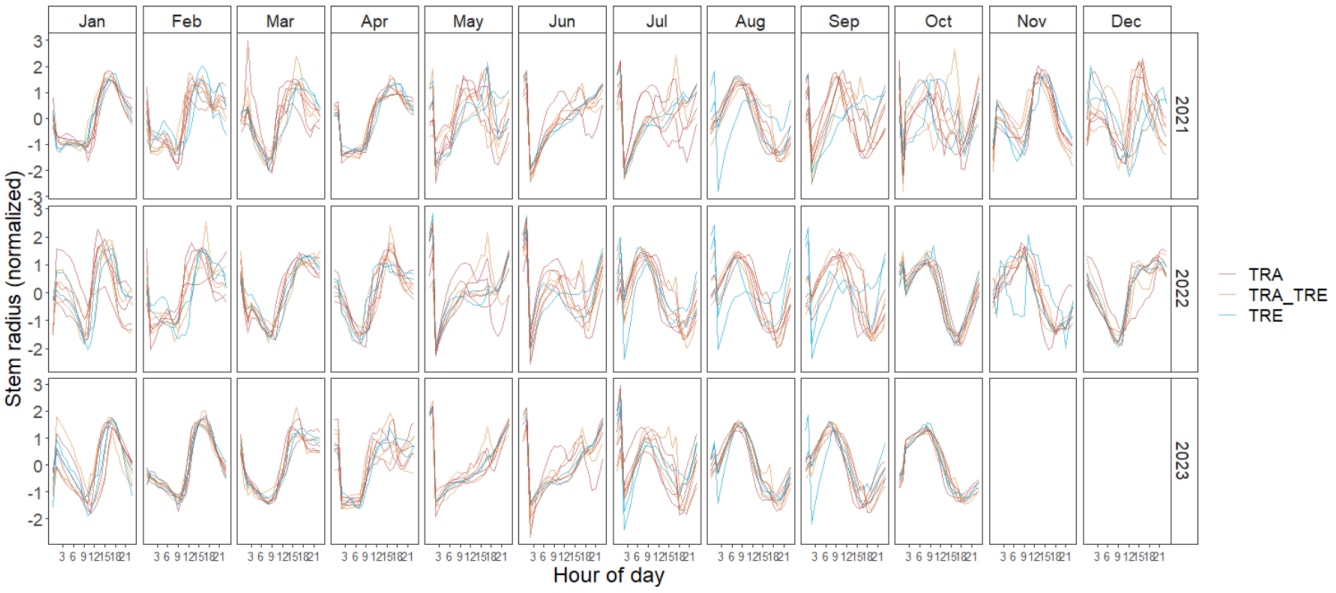

Figure 5. The hourly stem radius normalized between trees and averaged by month, with each solid line representing an individual tree in the forest (TRA), transition to the treeline (TRA-TRE), and treeline (TRE) zones.

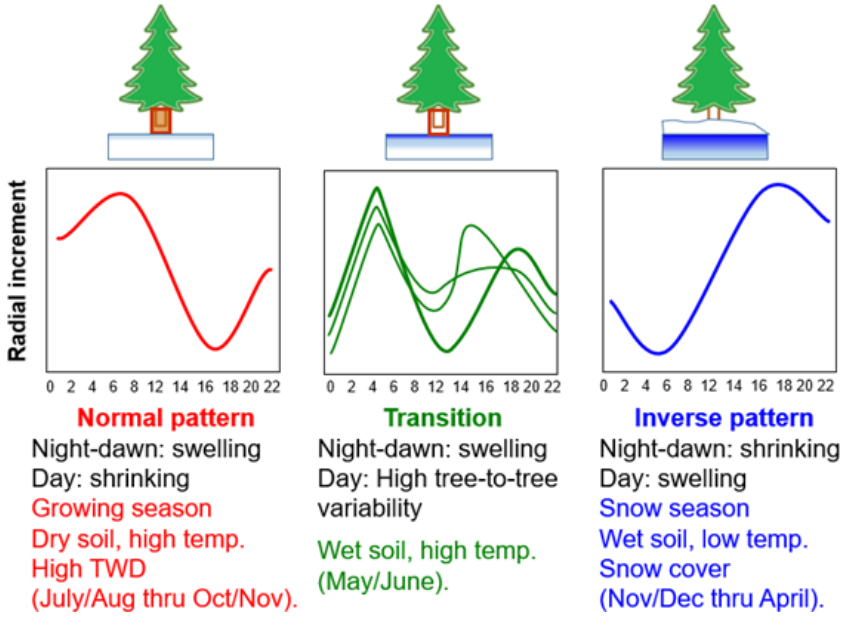

Figure 6. Graphic summarizing the patterns found in this study and showing the shifts in the snow and climate conditions and the swelling–shrinking stem cycles along the growing season. The rectangle around the trunk highlights that the tree is growing radially under the normal pattern and transitioning to a non-growing state during the transition phase.

ing, which can be interpreted as a response to climate warming. In addition, dates of growth onset are inferred from dendrometer data, but they should be confirmed using periodic wood monitoring and xylogenesis analyses (e.g., Sanmiguel-Vallelado et al., 2021). Unfortunately, we were prevented by the number of sample trees in each zone from drawing robust conclusions, so a good starting point for another study would be to extend the tree-ring chronologies to discern whether trees are becoming more or less responsive to growing season precipitation.

In agreement with prior studies, we observed that warmer February temperatures, specifically soil temperatures, enhanced overall growth and increased spring growth rates, and this positive effect was related to an earlier snow meltout and thus a longer growing season. The characteristic circadian cycle of stem increment that leads to wood production, de-

fined by night swelling and day shrinking, was detected in summer and fall (approximately from July to November) during the growing season. However, this pattern was inverted during the snow season (approximately from November to April), prior to the onset of growth (Fig. 6). Air temperature, soil temperature, and the presence of snow are strong indicators of how much and for how long trees can grow each year and cause the shift in daily stem increment patterns of tree radii.

Appendix A

Table A1. Tree features (DBH, height, and location).

Tree no.	DBH (cm)	Height (m)	Location	Location
311	18.9	14.6	TRA	Forest
326	19.0	15.0	TRA	Forest
306	14.0	13.2	TRA	Forest
316	18.4	14.0	TRA	Forest
314	14.7	11.0	TRA-TRE	Transition
304	12.2	8.5	TRA-TRE	Transition
798	12.7	9.0	TRA-TRE	Transition
799	20.0	6.0	TRE	Treeline
800	8.6	2.8	TRE	Treeline

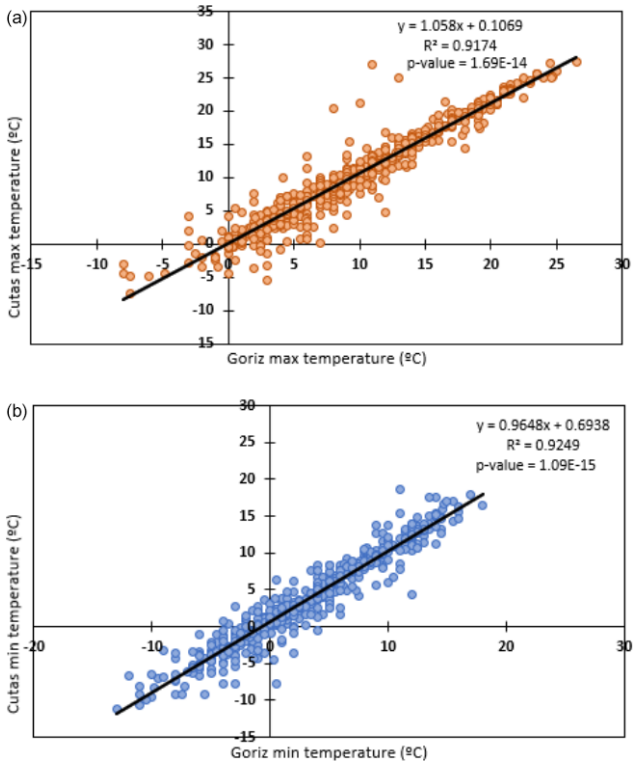

Figure A1. **(a)** Maximum and **(b)** minimum daily temperatures at Las Cutas (treeline site) and the Góriz refuge (local station).

Code availability. The code used in the analysis of this research is available upon request from the first author.

Data availability. The data used in this research are available upon request from the first author.

Author contributions. Conceptualization: JJC, ASV, HF, and JILM. Data curation and management: HF, JJC, ASV, and FRH. Formal analysis: HF, JJC, and ASV. Methodology: ASV, JJC, HF, and PDA. Resources: JILM, JJC, and JR. Writing – original draft preparation: HF. Writing – review and editing: HF, ASV, JJC, JILM, JR, FRH, and PDA. Visualization: JJC, HF, and ASV. Project administration: JILM, JJC, and JR.

Competing interests. The contact author has declared that none of the authors has any competing interests.

Disclaimer. Publisher's note: Copernicus Publications remains neutral with regard to jurisdictional claims made in the text, published maps, institutional affiliations, or any other geographical representation in this paper. While Copernicus Publications makes every effort to include appropriate place names, the final responsibility lies with the authors.

Special issue statement. This article is part of the special issue "Treeline ecotones under global change: linking spatial patterns to ecological processes". It is not associated with a conference.

Acknowledgements. The authors would like to thank the members of CryoPyr for carrying out the fieldwork, the Agencia Estatal de Meteorología of Spain for providing the Góriz refuge data, and the Pyrenees Institute of Ecology (Saragossa) for hosting Helen Flynn.

Financial support. This research was funded by a Fulbright Spain Predoctoral Fellowship to Helen Flynn. Alba Sanmiguel-Vallelado was supported by postdoctoral grant no. JDC2022-048316-I funded by MICIU/AEI/10.13039/501100011033 and by the European Union NextGenerationEU/PRTR.

The article processing charges for this open-access publication were covered by the CSIC Open Access Publication Support Initiative through its Unit of Information Resources for Research (URICI).

Review statement. This paper was edited by Matteo Garbarino and reviewed by Edurne Martinez Del Castillo and one anonymous referee.

References

Albrich, K., Rammer, W., and Seidl, R.: Climate change causes critical transitions and irreversible alterations of mountain forests, Glob. Change Biol., 26, 4013–4027, https://doi.org/10.1111/gcb.15118, 2020.

Andrus, R. A., Harvey, B. J., Rodman, K. C., Hart, S. J., and Veblen, T. T.: Moisture availability limits subalpine tree establishment, Ecology, 99, 567–575, https://doi.org/10.1002/ecy.2134, 2018.

Bunn, A., Korpela, M., Biondi, F., Campelo, F., Mérian, P., Qeadan, F., and Zang, C.: dplR: dendrochronology program library in R, [code], https://cran.r-project.org/package=dplR (last access: 26 February 2025), 2023.

Bunn, A. G.: A dendrochronology program library in R (dplR), Dendrochronologia, 26, 115–124, https://doi.org/10.1016/j.dendro.2008.01.002, 2008.

Bunn, A. G.: Statistical and visual crossdating in R using the dplR library, Dendrochronologia, 28, 251–258, https://doi.org/10.1016/j.dendro.2009.12.001, 2010.

Camarero, J. J., Guerrero-Campo, J., and Gutiérrez, E.: Tree-Ring Growth and Structure of Pinus uncinata and Pinus sylvestris in the Central Spanish Pyrenees, Arct. Alp. Res., 30, 1–10, https://doi.org/10.2307/1551739, 1998.

Cornes, R. C., van der Schrier, G., van den Besselaar, E. J. M., and Jones, P. D.: An Ensemble Version of the E-OBS Temperature and Precipitation Data Sets, J. Geophys. Res.-Atmos., 123, 9391–9409, https://doi.org/10.1029/2017JD028200, 2018.

Deslauriers, A., Rossi, S., and Anfodillo, T.: Dendrometer and intra-annual tree growth: What kind of information can be inferred?, Dendrochronologia, 25, 113–124, https://doi.org/10.1016/j.dendro.2007.05.003, 2007.

Dobbert, S., Pape, R., and Löffler, J.: The application of dendrometers to alpine dwarf shrubs – a case study to investigate stem growth responses to environmental conditions, Biogeosciences, 19, 1933–1958, https://doi.org/10.5194/bg-19-1933-2022, 2022.

Fritz, H. C.: Tree rings and climate, Academic Press Inc., London, ISBN-10 0122684508, 1976.

Galván, J. D., Camarero, J. J., and Gutiérrez, E.: Seeing the trees for the forest: drivers of individual growth responses to climate in inus uncinata mountain forests, J. Ecol., 102, 1244–1257, https://doi.org/10.1111/1365-2745.12268, 2014.

Gascoin, S., Hagolle, O., Huc, M., Jarlan, L., Dejoux, J.-F., Szczypta, C., Marti, R., and Sánchez, R.: A snow cover climatology for the Pyrenees from MODIS snow products, Hydrol. Earth Syst. Sci., 19, 2337–2351, https://doi.org/10.5194/hess-19-2337-2015, 2015.

Grossiord, C., Ulrich, D. E. M., and Vilagrosa, A.: Controls of the hydraulic safety–efficiency trade-off, Tree Physiol., 40, 573–576, https://doi.org/10.1093/treephys/tpaa013, 2020.

Hagedorn, F., Shiyatov, S. G., Mazepa, V. S., Devi, N. M., Grigor'ev, A. A., Bartysh, A. A., Fomin, V. V., Kapralov, D. S., Terent'ev, M., Bugman, H., Rigling, A., and Moiseev, P. A.: Treeline advances along the Urals mountain range – driven by improved winter conditions?, Glob. Change Biol., 20, 3530–3543, https://doi.org/10.1111/gcb.12613, 2014.

Harpold, A. A. and Molotch, N. P.: Sensitivity of soil water availability to changing snowmelt timing in the western U.S., Geophys. Res. Lett., 42, 8011–8020, https://doi.org/10.1002/2015GL065855, 2015.

Hedstrom, N. R. and Pomeroy, J. W.: Measurements and modelling of snow interception in the boreal forest, Hydrol. Process., 12, 1611–1625, https://doi.org/10.1002/(SICI)1099-1085(199808/09)12:10/11<1611::AID-HYP684>3.0.CO;2-4, 1998.

Holmes, R. L.: Computer-assisted quality control in tree-ring dating and measurement, Tree-Ring Bulletin, 43, 69–78, 1983.

Huang, M., Wang, G., Bie, X., Jiang, Y., Huang, X., Li, J.-J., Shi, S., Zhang, T., and Peng, P.-H.: Seasonal snow cover patterns explain alpine treeline elevation better than temperature at regional scale, Forest Ecosystems, 10, 100106, https://doi.org/10.1016/j.fecs.2023.100106, 2023.

Izagirre, E., Revuelto, J., Vidaller, I., Deschamps-Berger, C., Rojas-Heredia, F., Rico, I., Alonso-González, E., Gascoin, S., Serrano, E., and López-Moreno, J. I.: Pyrenean glaciers are disappearing fast: state of the glaciers after the extreme mass losses in 2022 and 2023, Reg. Environ. Change, 24, 172, https://doi.org/10.1007/s10113-024-02333-1, 2024.

Khorchani, M., Nadal-Romero, E., Lasanta, T., and Tague, C.: Carbon sequestration and water yield tradeoffs following restoration of abandoned agricultural lands in Mediterranean mountains, Environ. Res., 207, 112203, https://doi.org/10.1016/j.envres.2021.112203, 2022.

Knüsel, S., Peters, R. L., Haeni, M., Wilhelm, M., and Zweifel, R.: Processing and Extraction of Seasonal Tree Physiological Parameters from Stem Radius Time Series, Forests, 12, 765, https://doi.org/10.3390/f12060765, 2021.

Lázaro-Gimeno, D., Ferrari, C., Delhomme, N., Johansson, M., Sjölander, J., Singh, R. K., Mutwil, M., and Eriksson, M. E.: The circadian clock participates in seasonal growth in Norway spruce (Picea abies), Tree Physiol., 44, tpae139, https://doi.org/10.1093/treephys/tpae139, 2024.

López-Moreno, J. I.: Recent Variations of Snowpack Depth in the Central Spanish Pyrenees, Arct. Antarct. Alp. Res., 37, 253–260, https://doi.org/10.1657/1523-0430(2005)037[0253:RVOSDI]2.0.CO;2, 2005.

López-Moreno, J. I. and Latron, J.: Influence of canopy density on snow distribution in a temperate mountain range, Hydrol. Process., 22, 117–126, https://doi.org/10.1002/hyp.6572, 2008.

López-Moreno, J. I., Soubeyroux, J. M., Gascoin, S., Alonso-Gonzalez, E., Durán-Gómez, N., Lafaysse, M., Vernay, M., Carmagnola, C., and Morin, S.: Long-term trends (1958–2017) in snow cover duration and depth in the Pyrenees, Int. J. Climatol., 40, 6122–6136, https://doi.org/10.1002/joc.6571, 2020.

Lüttge, U. and Hertel, B.: Diurnal and annual rhythms in trees, Trees, 23, 683–700, https://doi.org/10.1007/s00468-009-0324-1, 2009.

Maxwell, R. S. and Larsson, L.-A.: Measuring tree-ring widths using the CooRecorder software application, Dendrochronologia, 67, 125841, https://doi.org/10.1016/j.dendro.2021.125841, 2021.

Mei-Jun, L. I. U., Qiu-Wen, C., Jin-Lin, L., Guo-Qing, L. I., and Sheng, D. U.: Seasonal dynamics of radial growth and micro-variation in stems of Quercus mongolica var. liaotungensis and Robinia pseudoacacia in loess hilly region, Chinese Journal of Plant Ecology, 47, 227–237, https://doi.org/10.17521/cjpe.2022.0100, 2023.

Noguera, I., Vicente-Serrano, S. M., Peña-Angulo, D., Domínguez-Castro, F., Juez, C., Tomás-Burguera, M., Lorenzo-Lacruz,

J., Azorin-Molina, C., Halifa-Marín, A., Fernández-Duque, B., and El Kenawy, A.: Assessment of vapor pressure deficit variability and trends in Spain and possible connections with soil moisture, Atmos. Res., 285, 106666, https://doi.org/10.1016/j.atmosres.2023.106666, 2023.

Pardo, I., Camarero, J. J., Gutiérrez, E., and García, M. B.: Uncoupled changes in tree cover and field layer vegetation at two Pyrenean treeline ecotones over 11 years, Plant Ecol. Divers., 6, 355–364, https://doi.org/10.1080/17550874.2013.811306, 2013.

Pepin, N., Bradley, R. S., Diaz, H. F., Baraer, M., Caceres, E. B., Forsythe, N., Fowler, H., Greenwood, G., Hashmi, M. Z., Liu, X. D., Miller, J. R., Ning, L., Ohmura, A., Palazzi, E., Rangwala, I., Schöner, W., Severskiy, I., Shahgedanova, M., Wang, M. B., Williamson, S. N., Yang, D. Q., and Mountain Research Initiative EDW Working Group: Elevation-dependent warming in mountain regions of the world, Nat. Clim. Change, 5, 424–430, https://doi.org/10.1038/nclimate2563, 2015.

Peterson, D. L.: Climate, limiting factors and environmental change in high-altitude forests of Western North America, in: The Impacts of Climate Variability on Forests, edited by: Beniston, M. and Innes, J. L., Springer, Berlin, Heidelberg, 191–208, https://doi.org/10.1007/BFb0009773, 1998.

Pomeroy, J. W., Gray, D. M., Hedstrom, N. R., and Janowicz, J. R.: Prediction of seasonal snow accumulation in cold climate forests, Hydrol. Process., 16, 3543–3558, https://doi.org/10.1002/hyp.1228, 2002.

Pomeroy, J. W., Bewley, D. S., Essery, R. L. H., Hedstrom, N. R., Link, T., Granger, R. J., Sicart, J. E., Ellis, C. R., and Janowicz, J. R.: Shrub tundra snowmelt, Hydrol. Process., 20, 923–941, https://doi.org/10.1002/hyp.6124, 2006.

Ren, P., Ziaco, E., Rossi, S., Biondi, F., Prislan, P., and Liang, E.: Growth rate rather than growing season length determines wood biomass in dry environments, Agr. Forest Meteorol., 271, 46–53, https://doi.org/10.1016/j.agrformet.2019.02.031, 2019.

Revuelto, J., López-Moreno, J. I., Azorin-Molina, C., and Vicente-Serrano, S. M.: Canopy influence on snow depth distribution in a pine stand determined from terrestrial laser data, Water Resour. Res., 51, 3476–3489, https://doi.org/10.1002/2014WR016496, 2015.

Revuelto, J., Azorin-Molina, C., Alonso-González, E., Sanmiguel-Vallelado, A., Navarro-Serrano, F., Rico, I., and López-Moreno, J. I.: Meteorological and snow distribution data in the Izas Experimental Catchment (Spanish Pyrenees) from 2011 to 2017, Earth Syst. Sci. Data, 9, 993–1005, https://doi.org/10.5194/essd-9-993-2017, 2017.

Saavedra, F. A., Kampf, S. K., Fassnacht, S. R., and Sibold, J. S.: Changes in Andes snow cover from MODIS data, 2000–2016, The Cryosphere, 12, 1027–1046, https://doi.org/10.5194/tc-12-1027-2018, 2018.

Sanmiguel-Vallelado, A., Camarero, J. J., Gazol, A., Morán-Tejeda, E., Sangüesa-Barreda, G., Alonso-González, E., Gutiérrez, E., Alla, A. Q., Galván, J. D., and López-Moreno, J. I.: Detecting snow-related signals in radial growth of *Pinus uncinata* mountain forests, Dendrochronologia, 57, 125622, https://doi.org/10.1016/j.dendro.2019.125622, 2019.

Sanmiguel-Vallelado, A., Camarero, J. J., Morán-Tejeda, E., Gazol, A., Colangelo, M., Alonso-González, E., and López-Moreno, J. I.: Snow dynamics influence tree growth by controlling soil temperature in mountain pine forests, Agr. Forest Meteorol., 296, 108205, https://doi.org/10.1016/j.agrformet.2020.108205, 2021.

Serrano-Notivoli, R., Tejedor, E., Sarricolea, P., Meseguer-Ruiz, O., de Luis, M., Saz, M. Á., Longares, L. A., and Olcina, J.: Unprecedented warmth: A look at Spain's exceptional summer of 2022, Atmos. Res., 293, 106931, https://doi.org/10.1016/j.atmosres.2023.106931, 2023.

Storck, P., Lettenmaier, D. P., and Bolton, S. M.: Measurement of snow interception and canopy effects on snow accumulation and melt in a mountainous maritime climate, Oregon, United States, Water Resour. Res., 38, 5-1–5-16, https://doi.org/10.1029/2002WR001281, 2002.

Tardif, J., Camarero, J. J., Ribas, M., and Gutiérrez, E.: Spatiotemporal Variability in Tree Growth in the Central Pyrenees: Climatic and Site Influences, Ecol. Monogr., 73, 241–257, https://doi.org/10.1890/0012-9615(2003)073[0241:SVITGI]2.0.CO;2, 2003.

Tumajer, J., Scharnweber, T., Smiljanic, M., and Wilmking, M.: Limitation by vapour pressure deficit shapes different intra-annual growth patterns of diffuse- and ring-porous temperate broadleaves, New Phytol., 233, 2429–2441, https://doi.org/10.1111/nph.17952, 2022.

Vicente-Serrano, S. M., Peña-Angulo, D., Murphy, C., López-Moreno, J. I., Tomas-Burguera, M., Domínguez-Castro, F., Tian, F., Eklundh, L., Cai, Z., Alvarez-Farizo, B., Noguera, I., Camarero, J. J., Sánchez-Salguero, R., Gazol, A., Grainger, S., Conradt, T., Boincean, B., and El Kenawy, A.: The complex multi-sectoral impacts of drought: Evidence from a mountainous basin in the Central Spanish Pyrenees, Sci. Total Environ., 769, 144702, https://doi.org/10.1016/j.scitotenv.2020.144702, 2021.

Villalba, R., Veblen, T. T., and Ogden, J.: Climatic Influences on the Growth of Subalpine Trees in the Colorado Front Range, Ecology, 75, 1450–1462, https://doi.org/10.2307/1937468, 1994.

Wigley, T. M. L., Briffa, K. R., and Jones, P. D.: On the Average Value of Correlated Time Series, with Applications in Dendroclimatology and Hydrometeorology, Cover Journal of Applied Meteorology and Climatology J. Appl. Meteorol. Clim., 23, 201–213, https://doi.org/10.1175/1520-0450(1984)023<0201:OTAVOC>2.0.CO;2, 1984.

Yang, J. C., Bowling, D. R., Smith, K. R., Kunik, L., Raczka, B., Anderegg, W. R. L., Bahn, M., Blanken, P. D., Richardson, A. D., Burns, S. P., Bohrer, G., Desai, A. R., Arain, M. A., Staebler, R. M., Ouimette, A. P., Munger, J. W., and Litvak, M. E.: Forest carbon uptake as influenced by snowpack and length of photosynthesis season in seasonally snow-covered forests of North America, Agr. Forest Meteorol., 353, 110054, https://doi.org/10.1016/j.agrformet.2024.110054, 2024.

Zang, C. and Biondi, F.: treeclim: an R package for the numerical calibration of proxy-climate relationships, Ecography, 38, 431–436, 2015.

Ziaco, E. and Biondi, F.: Stem Circadian Phenology of Four Pine Species in Naturally Contrasting Climates from Sky-Island Forests of the Western USA, Forests, 9, 396, https://doi.org/10.3390/f9070396, 2018.

Zweifel, R., Haeni, M., Buchmann, N., and Eugster, W.: Are trees able to grow in periods of stem shrinkage?, New Phytol., 211, 839–849, https://doi.org/10.1111/nph.13995, 2016.

Zweifel, R., Sterck, F., Braun, S., Buchmann, N., Eugster, W., Gessler, A., Häni, M., Peters, R. L., Walthert, L., Wilhelm, M., Ziemińska, K., and Etzold, S.: Why trees grow at night, New Phytol., 231, 2174–2185, https://doi.org/10.1111/nph.17552, 2021.